



Stability of active trapdoors in axisymmetry

Suraparb Keawsawasvong^a, Jim Shiau^{b,*}

^a *Department of Civil Engineering, Thammasat School of Engineering, Thammasat University, Pathumthani 12120, Thailand*

^b *School of Civil Engineering and Surveying, University of Southern Queensland, QLD 4350, Australia*

Received 8 February 2021; received in revised form 26 April 2021; accepted 1 May 2021

Abstract

Trapdoor stability has been widely studied by many researchers in the field of tunneling engineering. A general question being frequently asked is that why most sinkholes have a near-perfect circular shape on the ground surface. This could be possibly explained by the current numerical study using finite element limit analysis under axisymmetric condition, where upper and lower bound solutions of active circular trapdoors are determined. The failure study of sinkholes and the associated failure mechanisms in this paper are for non-homogeneous clay with a linear increase of strength with depth under various cover depth ratios and dimensionless strength gradients. A design equation for predicting the stability solutions is also developed based on the novel three dimensional solutions using axisymmetry.

Keywords: Numerical analysis; Axisymmetry; Stability; Trapdoor; Active failure

1 Introduction

Terzaghi (1936) pioneered the study on the stress distribution of a trapdoor by using a laboratory experiment. The study has been widely used as a benchmark solution in theoretical geomechanics, which can be extensively used in many applications in the field of geotechnical engineering. Since then, the problem of trapdoor stability has received much attention from many researchers. Two modes of failure mechanisms are of main concern: namely the active and the passive ones. Active failure is referred to the collapse of a trapdoor under its own weight and other external forces such as surcharge pressures. On the other hand, the passive failure of a trapdoor is initiated by external forces only.

The problem of active failures can be applied to several geotechnical engineering works such as the gravitational flow of granular material through hoppers (e.g., Jenike, 1964; Enstad, 1975), the underground roof in mining works (e.g., Fraldi & Guarracino, 2009; Suchowerska et al.,

2012), the stability of sinkhole problems (e.g., Augarde et al., 2003; Keawsawasvong & Ukritchon, 2019; Shiau & Hassan, 2020; Keawsawasvong, 2021), and the stability of tunnel problems (e.g., Keawsawasvong & Ukritchon, 2020; Shiau & Al-Asadi, 2020a; 2020b, 2020c, 2021; Ukritchon & Keawsawasvong, 2017, 2019a, 2019b, 2019c, 2019d, 2020; Ukritchon et al., 2017). For the problem of passive failures, Merifield et al. (2001) and Merifield and Sloan (2006) presented plastic solutions of the pullout capacity of plate anchors. Shiau & Al-Asadi (2020b, 2020c, 2021) studied the blowout stability of three dimensional (3D) tunnel headings.

In the past few decades, several works relating to the stability of active trapdoors were studied by using physical model tests (e.g., Terzaghi, 1936; Costa et al., 2009; Ladanyi & Hoyaux, 1969; Vardoulakis et al., 1981; Tanaka & Sakai, 1993; Santichaiant, 2002; Iglesia et al., 2011, 2013) and numerical or analytical methods (Terzaghi, 1943; Davis, 1968; Gunn, 1980; Vardoulakis et al., 1981; Koutsabeloulis & Griffiths, 1989; Sloan et al., 1990; Santichaiant, 2002; Martin, 2009; Keawsawasvong & Ukritchon, 2017, 2021; Wang et al.,

* Corresponding author.

E-mail address: jim.shiau@usq.edu.au (J. Shiau).

2017; Shiau & Hassan, 2020; Shiau & Sams, 2019; Keawsawasvong & Likitlersuang, 2021). It was noted from the literature that most numerical solutions of the trapdoor problem are concerned with planar trapdoors under plane strain conditions. However, very few studies were found in relation to the 3D study. Recently, the stability of 3D rectangular trapdoors in homogeneous clay was considered by Ukritchon et al. (2019), while Shiau et al. (2021) have also proposed rigorous 3D stability solutions of the square and circular trapdoors in homogeneous clay.

To the best of our knowledge, none can be found in relation to the stability study of 3D circular trapdoors in non-homogenous clay. This paper aims to present stability solutions of 3D circular trapdoors in non-homogenous clay with linearly increasing undrained shear strength by using the finite element limit analysis (FELA) under axisymmetric conditions. Nonlinear regression analysis is employed to perform a closed-form solution, and a design equation for the circular trapdoor problem is developed based on the FELA upper and lower bounds. The proposed closed-form expressions serve as a convenient tool to accurately determine the stability solutions for circular trapdoors under active failure mode.

2 Problem definition

Figure 1 shows the problem definition of an active circular trapdoor in non-homogenous clay with linearly increasing undrained shear strength under axisymmetric conditions. The circular trapdoor with the diameter (D) is located under a clay layer with the cover depth (H). The

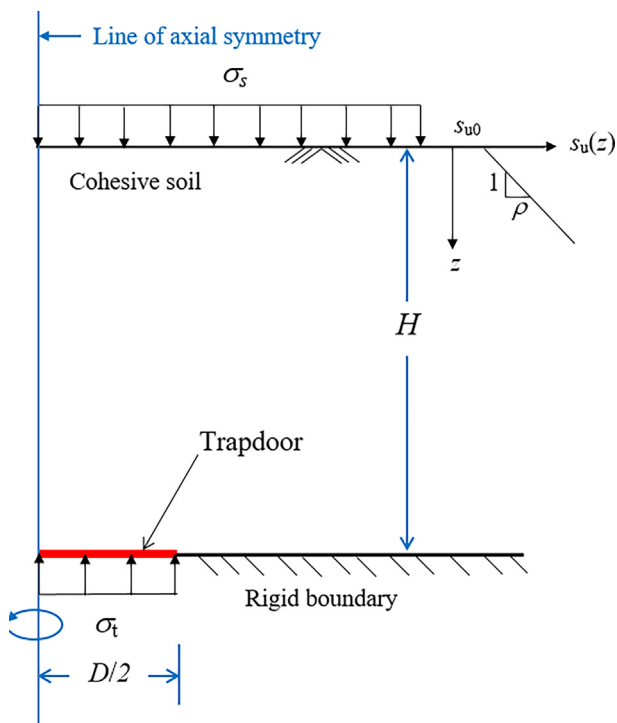


Fig. 1. Active circular trapdoor under an axisymmetric condition.

undrained shear strength of clay (s_u), increases linearly with the depth (z), $s_u = s_{u0} + \rho z$, where the undrained shear strength at the ground surface is denoted by s_{u0} and the strength gradient is denoted by ρ . A rigid-perfectly plastic Tresca material with the associated flow rule is used as a failure criterion for the material. Note that the constant unit weight of clay is represented by γ .

At the ground surface, there is a uniform surcharge (σ_s) applied over the surface, while a uniform trapdoor pressure (σ_t) is applied externally to support the soils above the trapdoor. The active failure is launched by setting the trapdoor to move downwards by the actions of σ_s and γ that is to be resisted by σ_t .

Using the concept of dimensionless ratios for practical design purposes, the stability solutions of active circular trapdoors in non-homogenous clay with linearly increasing undrained shear strength are determined through the use of two dimensionless variables as shown in Eq. (1).

$$N = \frac{\sigma_s + \gamma H - \sigma_t}{s_{u0}} = f\left(\frac{H}{D}, \frac{\rho H}{s_{u0}}\right), \tag{1}$$

where N is the stability number and it is a function of H/D and $\rho H/s_{u0}$. Note that H/D is the cover depth ratio and $\rho H/s_{u0}$ is the dimensionless strength gradient. The negative sign in front of σ_t represents the action of the resistance whereas the positive signs of σ_s and γ represent the “active” action of the driving stresses. A wide range of dimensionless parameters H/D and $\rho H/s_{u0}$ used in the current study are shown in Table 1.

3 Method of analysis

Finite element limit analysis (FELA) is rigorous and powerful when both upper bound (UB) and lower bound (LB) estimates can bracket the true collapse load (Sloan, 2013). The underlying bound theorems assume a rigid-perfectly plastic material with associated plasticity. The initial developments of FELA using linear programming were proposed by Sloan (1988, 1989). The newer developments are based on a much faster nonlinear programming formulation by (Lyamin and Sloan (2002a, 2002b)) and Krabbenhoft et al. (2007). OptumG2 (Krabbenhoft et al., 2015), a commercially available FELA software, was used to derive the upper and lower bound solutions of active circular trapdoors in non-homogeneous clay. Figure 2(a) shows the numerical model of a circular trapdoor under axisymmetric conditions. The centerline of the problem is set to be the line of axial symmetry located at the left of the domain. The soil mass above the trapdoor is represented by a Tresca material with an associated flow rule.

Table 1
List of dimensionless parameters used in the study.

Dimensionless parameter	Values
H/D	0.5, 1, 2, 4, 8, and 10
$\rho H/s_{u0}$	0, 0.25, 0.5, 0.75, 1, 2, and 4

The trapdoor is modelled as rigid plate elements under rough surface conditions. Owing to the large stress and velocity discontinuities at the corner of the trapdoor, a short vertical line is introduced using interface elements is added to the corner of the trapdoor as shown in Fig. 2 (b). The undrained shear strength of the interface elements is set to be zero. Note that this vertical line in Fig. 2(b) is very important in the UB analysis since velocity discontinuities are not allowed to occur along all inter-element edges but they are expected to take place at the corner of trapdoor, which can significantly improve the accuracy of the UB solutions. Nevertheless, this vertical line is not sensitive to the accuracy of LB solutions since stress discontinuities are modelled at all inter-

The boundary conditions of the axisymmetric problem are important. At the left-hand side (centerline) of the model, only vertical movement is allowed so as to represent the axisymmetric condition. The condition is the same as for the right-hand side (far side) boundary. At the bottom boundary of the model, both vertical and horizontal movements are not allowed. Noting that the size of the domain is chosen to be large enough in order to contain the plastic zone within the domain. It is also important that the overall velocity field is not allowed to intersect the right-hand side boundary for all simulations.

To determine the stability factor (N) in this study, the term γ in Eq. (1) is the objective function and is to be optimized using the gravity multiplier method in FELA. This is done by having both σ_s and σ_t terms be fixed as constant values due to the independency of loading direction in an undrained analysis where no volume change occurs during plastic shearing. In all analyses of the paper, a six-node triangular element is adopted for the upper bound analysis, where each node contains two unknown velocities that vary quadratically within the triangular element. The formulated objective function is to minimize the unit weight γ . In the lower bound analysis, a linear three-node triangular

element is used, where each node is associated with three unknown stresses. In contrast to the upper bound, the objective function of the lower bound analysis is to maximize the unit weight γ by using equilibrium equations, where stress boundary conditions and the yield criterion are satisfied.

The mesh adaptivity technique (Ciria et al., 2008) is a powerful feature for improving LB and UB solutions. By activating this feature, more elements are added to the sensitive regions with large shear strain gradients at any iteration step, aiming to bridge the differences between UB and LB solutions. In all analyses of this paper, five iterations of mesh adaptivity are adopted for all UB and LB simulations, with 5000–10,000 elements used in the iteration steps. It is interesting to note that the current technique reveals the location of a possible failure mechanism at the final stage of mesh adaptivity.

4 Results and comparisons

To the best of our knowledge, the non-homogeneous solution is the first of its kind in the circular trapdoor problem. Very few published results can be used for comparison purposes except the recent 3D work in Shiau et al. (2021) for a homogeneous solution. Figure 3 shows such a comparison for the homogeneous cases of $\rho H/s_{u0} = 0$. It is to be noted that the solutions from Shiau et al. (2021) are obtained from 3D UB and LB FELA, while the present study is derived by axisymmetric two dimensional (2D) UB and LB FELA. Interestingly, excellent agreement is found between the stability number N in the present study and those in Shiau et al. (2021). It should be noted that the differences between 3D UB solutions by Shiau et al. (2021) are larger than present 2D axisymmetric UB solutions about 0.5% to 5%. In addition, the differences between 3D LB solutions and present 2D LB solutions are in the range of 0.2% to 2%.

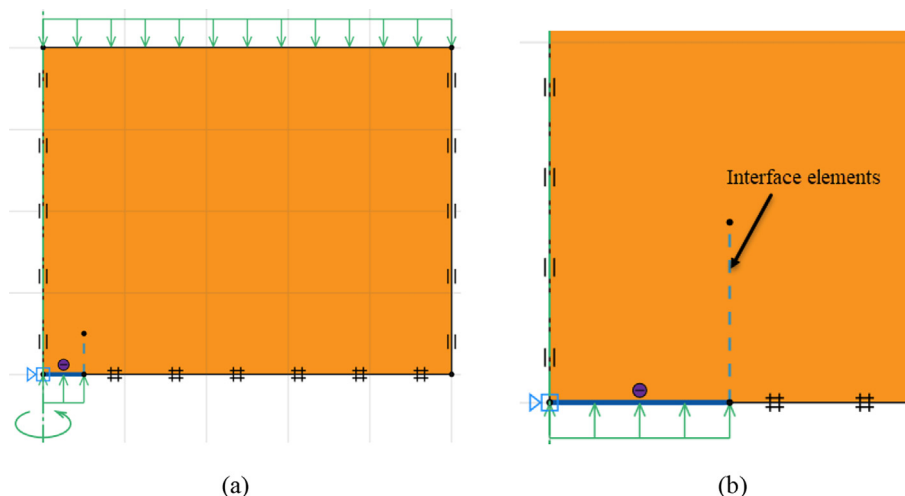


Fig. 2. (a) Numerical model of the undrained stability of an active circular trapdoor in OptumG2, and (b) interface elements.

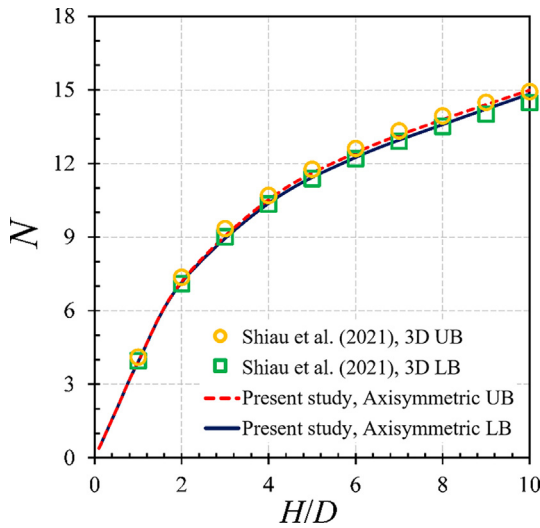


Fig. 3. Verification of undrained stability of an active circular trapdoor for the cases of $\rho H/s_{u0} = 0$.

The effect of the cover depth ratio (H/D) on the stability number (N) is shown in Fig. 4, where a nonlinear relationship between N and H/D is observed. An increase in H/D results in an increase in N for all values of $\rho H/s_{u0}$, and the rate of increase in N is greater as $\rho H/s_{u0}$ becomes larger. It should be noted that the exact values of N can be accurately bracketed by the computed upper and lower bound solutions within 1%.

Figure 5 shows the relationship between the dimensionless strength gradient ($\rho H/s_{u0}$) and the stability solutions (N). A linear relationship can be observed for all H/D ratios as shown in the figure. Also, note the increasing gradient as H/D becomes larger. Figure 6 presents a comparison of adaptive meshes and failure mechanisms for the various depth ratios $H/D = 0.5, 2, 6,$ and 10 ($\rho H/s_{u0} = 1$). Using the mesh adaptivity technique, more elements are added to the sensitive regions that have large shear strain

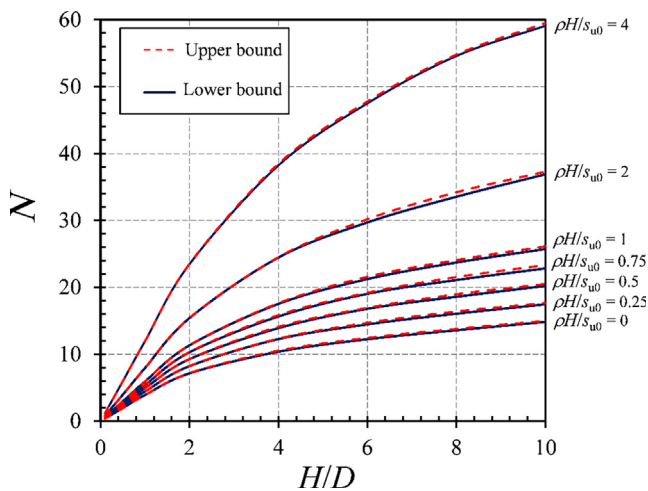


Fig. 4. Effect of H/D on the stability number N with various dimensionless strength gradients ($\rho H/s_{u0}$).

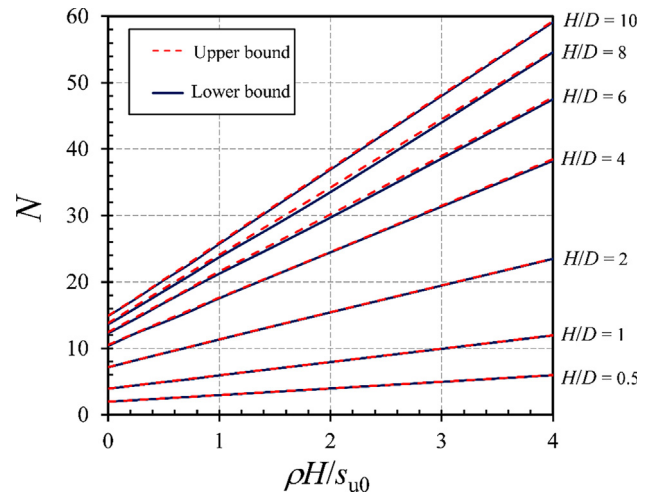


Fig. 5. Effect of $\rho H/s_{u0}$ on the stability number N with different cover depth ratios (H/D).

gradients. As stated by Martin (2011), those sensitive regions with very fine mesh refinement can reveal slip-line fields which can be considered as failure mechanisms of stability problems. For the very shallow trapdoors ($H/D = 0.5$ and 2), the plastic zones are extended vertically from the corner of the trapdoor to the ground surface, and there is little lateral expansion of the plastic zones across the soils above the trapdoor. For the intermediate and deep trapdoors with $H/D = 6$ and 10 , the plastic zones are laterally expanded in the horizontal direction, indicating a greater shearing resistance against active failures.

The effect of $\rho H/s_{u0}$ on adaptive meshes and failure mechanisms of active circular trapdoors is shown in Fig. 7 for the shallow case with $H/D = 2$, while in Fig. 8, the effect is for the deep case with $H/D = 10$. It can be found from Fig. 7 that an increase in $\rho H/s_{u0}$ results in an obvious decrease in the size of the plastic zones in the horizontal direction. The extent of ground surface failure also decreases as the value of $\rho H/s_{u0}$ increases. The same observation is found for the deep case with $H/D = 10$ in Fig. 8.

5 Discussions

5.1 Design equation

A design equation is developed by employing the average bound solutions and the method of curve fitting. This design equation consists of a linear function of $\rho H/s_{u0}$, and a nonlinear function of H/D . The best mathematic form of the design equation is shown in Eq. (2).

$$N = \frac{(\sigma_s + \gamma H - \sigma_t)}{s_{u0}} = \frac{a_1 \left(\frac{H}{D}\right)^{a_5}}{1 + a_2 \left(\frac{H}{D}\right)^{a_5}} + \left[\frac{a_3 \left(\frac{H}{D}\right)^{a_5}}{1 + a_4 \left(\frac{H}{D}\right)^{a_5}} \right] \left(\frac{\rho H}{s_{u0}} \right), \quad (2)$$

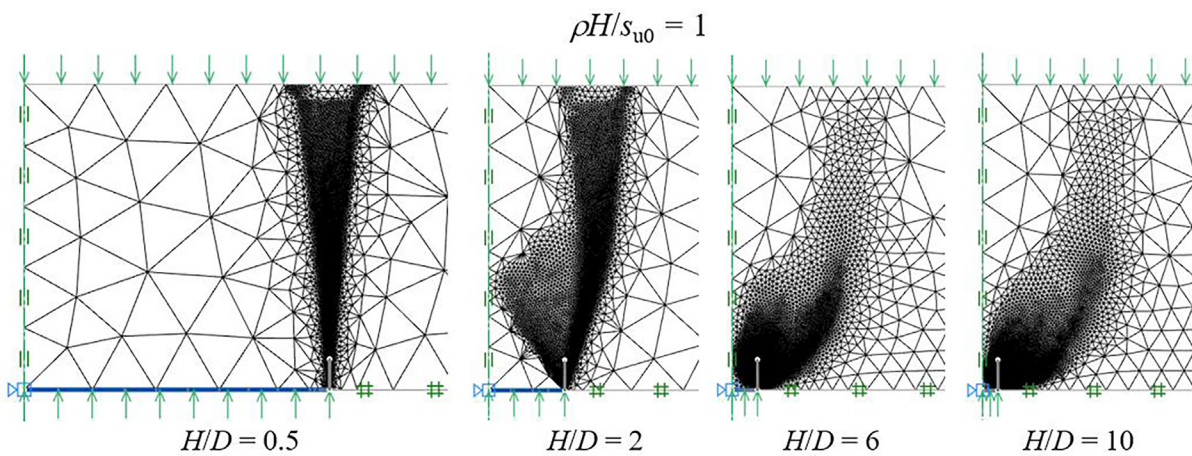


Fig. 6. Comparison of adaptive meshes and failure mechanisms ($\rho H/s_{u0} = 1$, $H/D = 0.5, 2, 6, 10$).

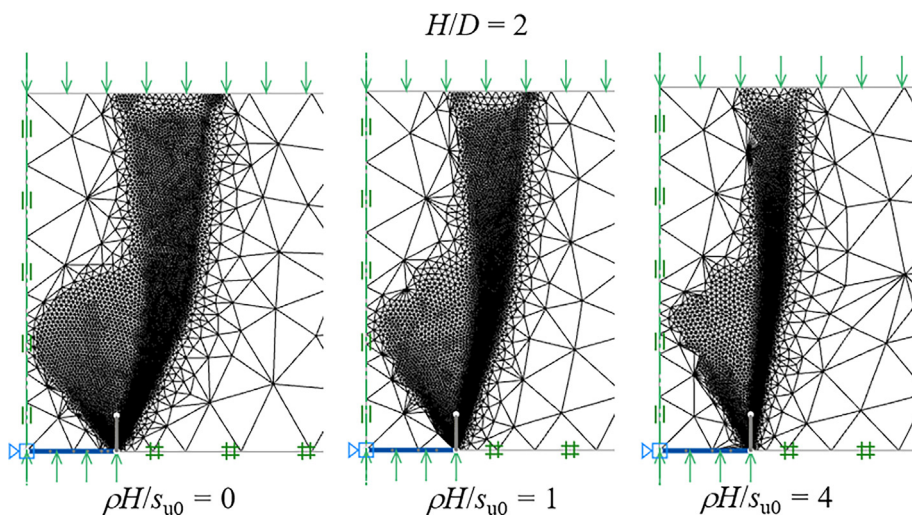


Fig. 7. Comparison of adaptive meshes and failure mechanisms ($H/D = 2$).

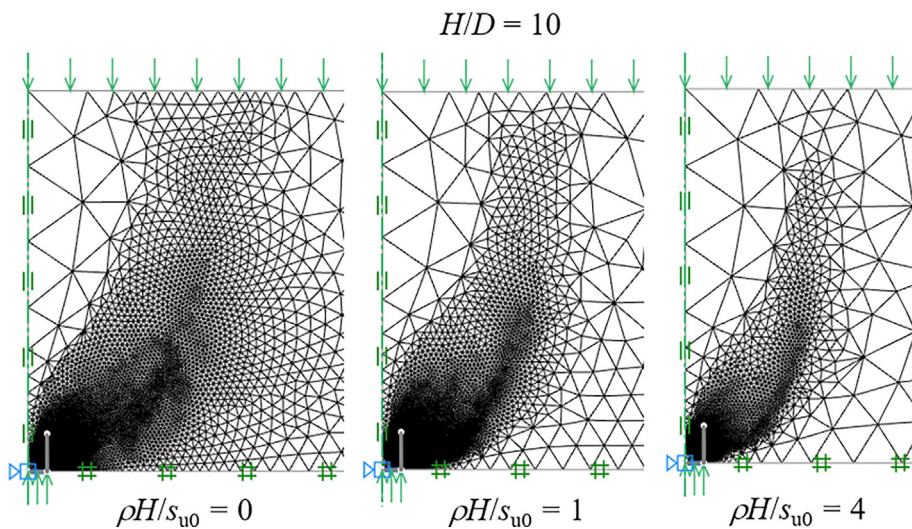


Fig. 8. Comparison of adaptive meshes and failure mechanisms ($H/D = 10$).

Table 2
Optimal value of statistical constants.

a_1	a_2	a_3	a_4	a_5
5.1074	0.2803	2.3919	0.1446	1.1569

where a_1 – a_5 are constant coefficients and they are presented in Table 2. By using the least square method (Sauer, 2014), the optimal values of these constant coefficients are obtained with very high accuracy. The coefficient of determination (R^2) is 99.98%, as shown in Fig. 9. Note that the parameters a_1 – a_5 are constant coefficients regardless of problem sizes and ranges of soil properties.

By multiplying s_{u0} to both sides in Eq. (2) and rearranging terms, a general form for predicting σ_t can be obtained as shown in Eq. (3).

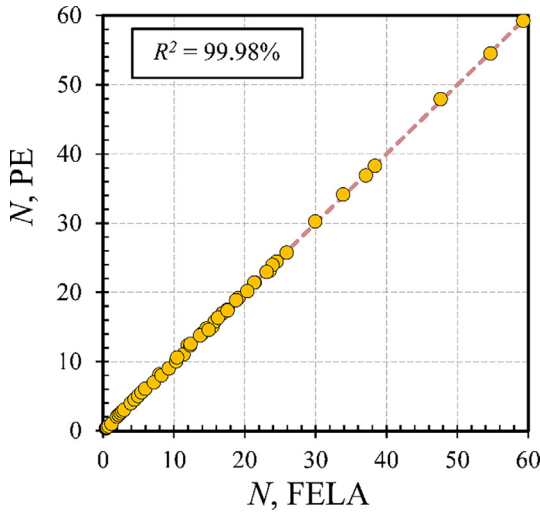


Fig. 9. Comparison of the results of N between the proposed equation (PE) and FELA.

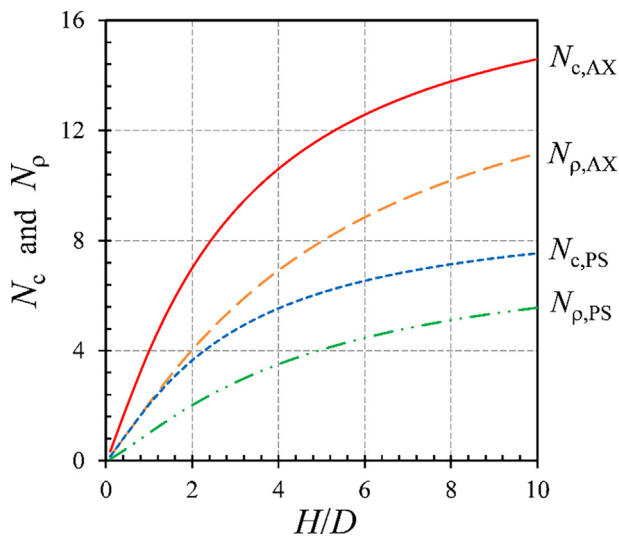


Fig. 10. Comparison of the stability factors N_c and N_ρ between plane strain (PS) and axisymmetric (AX) conditions.

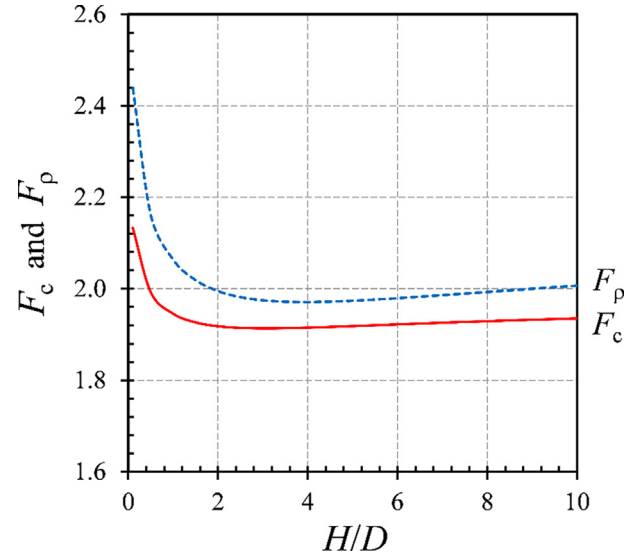


Fig. 11. Relationship between the shape factors F_c and F_ρ and the cover depth ratio (H/D).

$$\sigma_t = \sigma_s + \gamma H - N_c s_{u0} - N_\rho (\rho H), \tag{3}$$

$$\text{where } N_c = \frac{a_1 \left(\frac{H}{D}\right)^{a_5}}{1 + a_2 \left(\frac{H}{D}\right)^{a_5}} \text{ and } N_\rho = \frac{a_3 \left(\frac{H}{D}\right)^{a_5}}{1 + a_4 \left(\frac{H}{D}\right)^{a_5}}.$$

N_c and N_ρ are the stability factors to be used in Eq. (3) for estimating the supporting pressure σ_t , which can be either positive (compression) or negative (tension). With the chosen design parameters such as (H , D , s_{u0} , ρ , γ , σ_s), Eq. (3) can be used by engineers to estimate the required minimum supporting pressure (σ_t) to maintain soil stability of the circular trapdoors in the preliminary stage of design

5.2 Shape effect

The 3D shape effect is demonstrated by comparing the current axisymmetric results (AX) with those in Keawsawasvong and Ukritchon (2017) using plane strain (PS) conditions. Figure 10 shows the variations of the present axisymmetric stability factors $N_{c,AX}$ and $N_{\rho,AX}$ (Eq. (3)) and those plane strain stability factors $N_{c,PS}$ and $N_{\rho,PS}$ from Keawsawasvong and Ukritchon (2017). It can be seen from Fig. 10 that the axisymmetric stability factors are approximately two times higher than the plane strain ones. Axisymmetric analyses produce larger stability factors $N_{c,AX}$ and $N_{\rho,AX}$, therefore yielding small supporting pressures σ_t (Eq. (3)). Consequently, it is considered as a less conservative method.

Two shape factors, F_c and F_ρ , are presented in Fig. 11 to show the differences in results between AX and PS. They are defined as $F_c = (N_{c,AX}/N_{c,PS})$ and $F_\rho = (N_{\rho,AX}/N_{\rho,PS})$ respectively. All lines of F_c and F_ρ are in the range of 1.92 to 2.04 except for the shallow trapdoor with H/D being less than 1. It is not surprising to see that, for $H/D < 1$, much larger shape effect can be expected, as seen in Fig. 11.

6 Conclusions

This paper has successfully presented novel axisymmetric solutions for active circular trapdoors in non-homogeneous clays with a linear increase of strength with depth. By using the finite element limit analysis, the upper and lower bound solutions of the axisymmetric problem were derived based on two dimensionless parameters named the cover depth ratio (H/D) and the dimensionless strength gradient ($\rho H/s_{u0}$). An increase in both cover depth ratio and dimensionless strength gradient results in an increase in the stability solution. The relationship between the stability solution and the cover depth ratio is nonlinear while that of the stability solution and the dimensionless strength gradient is linear. The sizes of the failure mechanisms are found to be much dependent on the values of the cover depth ratio and the dimensionless strength gradient. The shape effect between 3D and 2D was also studied in the paper. In all analyses in the study, the stability solutions can be accurately bracketed by the computed bound solutions to within 1%. A design equation was developed by using nonlinear regression analysis of the average bound solutions. The equation is practical, and it is useful for engineers in their daily design work.

Declaration of Competing Interest

The authors declare that they have no known competing financial interests or personal relationships that could have appeared to influence the work reported in this paper.

References

- Augarde, C. E., Lyamin, A. V., & Sloan, S. W. (2003). Prediction of undrained sinkhole collapse. *Journal of Geotechnical and Geoenvironmental Engineering*, 129(3), 197–205.
- Ciria, H., Peraire, J., & Bonet, J. (2008). Mesh adaptive computation of upper and lower bounds in limit analysis. *International Journal for Numerical Methods in Engineering*, 75(8), 899–944.
- Costa, Y., Zornberg, J., Bueno, B., & Costa, C. (2009). Failure mechanisms in sand over a deep active trapdoor. *Journal of Geotechnical and Geoenvironmental Engineering*, 135(11), 1741–1753.
- Davis, E. H. (1968). Theories of plasticity and the failure of soil masses. In I. K. Lee (Ed.), *Soil Mechanics: Selected Topics* (pp. 341–380). London: Butterworths.
- Enstad, G. (1975). On the theory of arching in mass flow hoppers. *Chemical Engineering Science*, 30(10), 1273–1283.
- Fraldi, M., & Guarracino, F. (2009). Limit analysis of collapse mechanisms in cavities and tunnels according to the Hoek-Brown failure criterion. *International Journal of Rock Mechanics and Mining Sciences*, 46(4), 665–673.
- Gunn, M. J. (1980). Limit analysis of undrained stability problems using a very small computer. In *Proceedings of the Symposium on Computer Applications in Geotechnical Problems in Highway Engineering*, Cambridge.
- Iglesia, G. R., Einstein, H. H., & Whitman, R. V. (2011). Validation of centrifuge model scaling for soil systems via trapdoor tests. *Journal of Geotechnical and Geoenvironmental Engineering*, 137(11), 1075–1089.
- Iglesia, G., Einstein, H. H., & Whitman, R. V. (2013). Investigation of Soil Arching with Centrifuge Tests. *Journal of Geotechnical and Geoenvironmental Engineering*, 140(2), 04013005.
- Jenike, A. (1964). Steady gravity flow of frictional-cohesive solids in converging channels. *Journal of Applied Mechanics*, 31(1), 5–11.
- Keawsawasvong, S. (2021). Limit analysis solutions for spherical cavities in sandy soils under overloading. *Innovative Infrastructure Solutions*, 6(1), 33.
- Keawsawasvong, S., & Likitlersuang, S. (2021). Undrained stability of active trapdoors in two-layered clays in press. *Underground Space*. <https://doi.org/10.1016/j.undsp.2020.07.002>.
- Keawsawasvong, S., & Ukritchon, B. (2017). Undrained stability of an active planar trapdoor in non-homogeneous clays with a linear increase of strength with depth. *Computers and Geotechnics*, 81, 284–293.
- Keawsawasvong, S., & Ukritchon, B. (2019). Undrained stability of a spherical cavity in cohesive soils using finite element limit analysis. *Journal of Rock Mechanics and Geotechnical Engineering*, 11(6), 1274–1285.
- Keawsawasvong, S., & Ukritchon, B. (2020). Design equation for stability of shallow unlined circular tunnels in Hoek-Brown rock masses. *Bulletin of Engineering Geology and the Environment*, 79(8), 4167–4190.
- Keawsawasvong, S., & Ukritchon, B. (2021). Undrained stability of plane strain active trapdoors in anisotropic and non-homogeneous clays. *Tunnelling and Underground Space Technology*, 107, 103628.
- Koutsabeloulis, N. C., & Griffiths, D. V. (1989). Numerical modelling of the trap door problem. *Géotechnique*, 39(1), 77–89.
- Krabbenhoft, K., Lyamin, A., & Krabbenhoft, J. (2015). Optum computational engineering (OptumG2). Available on: <https://optumce.com/wp-content/uploads/2016/05/Theory.pdf>.
- Krabbenhoft, K., Lyamin, A. V., & Sloan, S. W. (2007). Formulation and solution of some plasticity problems as conic programs. *International Journal of Solids and Structures*, 44(5), 1533–1549.
- Ladanyi, B., & Hoyaux, B. (1969). A study of the trap-door problem in a granular mass. *Canadian Geotechnical Journal*, 6(1), 1–15.
- Lyamin, A. V., & Sloan, S. W. (2002a). Lower bound limit analysis using non-linear programming. *International Journal for Numerical Methods in Engineering*, 55(5), 573–611.
- Lyamin, A. V., & Sloan, S. W. (2002b). Upper bound limit analysis using linear finite elements and non-linear programming. *International Journal for Numerical and Analytical Methods in Geomechanics*, 26(2), 181–216.
- Martin, C. M. (2009). Undrained collapse of a shallow plane-strain trapdoor. *Géotechnique*, 59(10), 855–863.
- Martin, C. M. (2011). The use of adaptive finite element limit analysis to reveal slip-line fields. *Géotechnique Letters*, 1(2), 23–29.
- Merifield, R. S., Sloan, S. W., & Yu, H. S. (2001). Stability of plate anchors in undrained clay. *Géotechnique*, 51(2), 141–153.
- Merifield, R. S., & Sloan, S. W. (2006). The ultimate pullout capacity of anchors in frictional soils. *Canadian Geotechnical Journal*, 43(8), 852–868.
- Santichaiant, K. (2002). *Centrifuge modeling and analysis of active trapdoor in sand* [Doctoral dissertation], Department of Civil, Environmental and Architectural Engineering, University of Colorado at Boulder.
- Sauer, T. (2014). *Numerical Analysis*. UK: Pearson Education Limited.
- Shiau, J., & Al-Asadi, F. (2020a). Two-dimensional tunnel heading stability factors F_c , F_s and F_γ . *Tunnelling and Underground Space Technology*, 97, 103293.
- Shiau, J., & Al-Asadi, F. (2020b). Determination of critical tunnel heading pressures using stability factors. *Computers and Geotechnics*, 119, 103345.
- Shiau, J., & Al-Asadi, F. (2020c). Three-dimensional analysis of circular tunnel headings using Broms and Bennermarks' Original Stability Number. *International Journal of Geomechanics*, 20(7), 0001734.
- Shiau, J., & Al-Asadi, F. (2021). Twin tunnels stability factors F_c , F_s and F_γ . *Geotechnical and Geological Engineering*, 39(1), 335–345.
- Shiau, J., & Hassan, M. M. (2020). Undrained stability of active and passive trapdoors. *Geotechnical Research*, 7(1), 40–48.
- Shiau, J., Lee, J. S., & Al-Asadi, F. (2021). Three-dimensional stability analysis of active and passive trapdoors. *Tunnelling and Underground Space Technology*, 107, 103635.
- Shiau, J., & Sams, M. (2019). Relating volume loss and greenfield settlement. *Tunnelling and Underground Space Technology*, 83, 145–152.
- Sloan, S. W. (2013). Geotechnical stability analysis. *Géotechnique*, 63(7), 531–572.
- Sloan, S. W., Assadi, A., & Purushothaman, N. (1990). Undrained stability of a trapdoor. *Géotechnique*, 40(1), 45–62.

- Sloan, S. W. (1988). Lower bound limit analysis using finite elements and linear programming. *International Journal for Numerical and Analytical Methods in Geomechanics*, 12(1), 61–77.
- Sloan, S. W. (1989). Upper bound limit analysis using finite elements and linear programming. *International Journal for Numerical and Analytical Methods in Geomechanics*, 13(3), 263–282.
- Suchowerska, A. M., Merifield, R. S., Carter, J. P., & Clausen, J. (2012). Prediction of underground cavity roof collapse using the Hoek-Brown failure criterion. *Computers and Geotechnics*, 44, 93–103.
- Tanaka, T., & Sakai, T. (1993). Progressive failure and scale effect of trap-door problems with granular materials. *Soils and Foundations*, 33(1), 11–22.
- Terzaghi, K. (1936). Stress distribution in dry and saturated sand above a yielding trap-door. In *Proceedings, 1st International Conference on Soil Mechanics and Foundation Engineering*, Cambridge, Mass.
- Terzaghi, K. (1943). *Theoretical Soil Mechanics*. New York: Wiley.
- Ukritchon, B., & Keawsawasvong, S. (2017). Design equations for undrained stability of opening in underground walls. *Tunnelling and Underground Space Technology*, 70, 214–220.
- Ukritchon, B., & Keawsawasvong, S. (2019a). Stability of retained soils behind underground walls with an opening using lower bound limit analysis and second-order cone programming. *Geotechnical and Geological Engineering*, 37(3), 1609–1625.
- Ukritchon, B., & Keawsawasvong, S. (2019b). Lower bound solutions for undrained face stability of plane strain tunnel headings in anisotropic and non-homogeneous clays. *Computers and Geotechnics*, 112, 204–217.
- Ukritchon, B., & Keawsawasvong, S. (2019c). Stability of unlined square tunnels in Hoek-Brown rock masses based on lower bound analysis. *Computers and Geotechnics*, 105, 249–264.
- Ukritchon, B., & Keawsawasvong, S. (2019d). Lower bound stability analysis of plane strain headings in Hoek-Brown rock masses. *Tunnelling and Underground Space Technology*, 84, 99–112.
- Ukritchon, B., & Keawsawasvong, S. (2020). Undrained stability of unlined square tunnels in clays with linearly increasing anisotropic shear strength. *Geotechnical and Geological Engineering*, 38(1), 897–915.
- Ukritchon, B., Keawsawasvong, S., & Yingchaloenkitkhajorn, K. (2017). Undrained face stability of tunnels in Bangkok Subsoils. *International Journal of Geotechnical Engineering*, 11(3), 262–277.
- Ukritchon, B., Yoang, S., & Keawsawasvong, S. (2019). Three-dimensional stability analysis of the collapse pressure on flexible pavements over rectangular trapdoors. *Transportation Geotechnics*, 21, 100277.
- Vardoulakis, I., Graf, B., & Gudehus, G. (1981). Trap-door problem with dry sand: A statical approach based upon model kinematics. *International Journal for Numerical and Analytical Methods in Geomechanics*, 5(1), 57–78.
- Wang, L., Leshchinsky, B., Evans, T. M., & Xie, Y. (2017). Active and passive arching stress in $C-\Phi$ soils: A sensitivity study using computational limit analysis. *Computers and Geotechnics*, 84, 47–55.